

Photon Dose Calculations in a Fluence- Based Treatment Planning System

Data Processing, Implementation and Validation

Lars Weber

Department of Radiation Physics
The Jubileum Institute
Lund University, 2003



LUND UNIVERSITY

ISBN 91-628-5580-8

Printed in Sweden by Lund University, Media-Tryck, 2003

© Lars Weber (pp 1-51), 2003

Sol gi'r varme,
Sol gi'r sved,
Sol gi'r næsen fregner.

Sol står op
og sol går ned
osse når det regner.

Halfdan Rasmussen (1915 - 2002)

Abstract

The accuracy of dose calculations for various aspects of a treatment planning system (TPS) using an energy fluence beam modelling has been evaluated. The investigated TPS uses a beam model, which separates the energy fluence into a number of sources in the treatment head. The energy fluence components are transported towards the patient and, together with the scatter generated in the patient, yield the total dose. The parameters in the model on which the calculations are based are derived from measured data.

Several steps must be performed before a TPS can be adopted for clinical use. The most basic step is to collect the data required for the dose calculation algorithm of the TPS, such as depth doses, dose profiles, output factors in air and in water, etc. In this work, an investigation has been made of different methods of measuring output factors in air. An investigation on the variability of the prescribed characterisation measurements among several users has also been conducted.

The treatment unit characterisation step involves taking the measured input data, stated by the TPS vendor, and converting these into the model parameters required by the TPS dose calculation model. TPS-calculated dose distributions for the standard characterisation fields have been evaluated and compared with the input dose measurements. This constitutes the basic quality control level for the individual beams. In clinical settings, a variety of accessories in terms of field shaping, compensators, wedges, etc, are commonly used. These different treatment scenarios have been evaluated in terms of the level of accuracy achievable. For a number of situations, e.g. beams in heterogeneous media, modulated and asymmetric beams and beams subject to different scattering volumes, the TPS dose calculations have been compared with measured and Monte Carlo simulated data. With the exception of dose calculations in the build up region and for some 60-degree wedge data, the dose calculations agree with measurements to within 3 % level.

Key words: radiotherapy, quality assurance, treatment planning system, pencil kernel, point kernel, modulation

List of papers

This thesis is based on the following papers, which will be referred to by their Roman numerals:

- I. Knöös T, Ahnesjö A, Nilsson P, **Weber L** 1995 Limitations of a pencil beam approach to photon dose calculations in lung tissue *Phys Med Biol* **40** 1411-1420
- II. **Weber L**, Ahnesjö A, Nilsson P, Saxner M, Knöös T 1996 Verification and implementation of dynamic wedge calculations in a treatment planning system based on a dose-to-energy-fluence formalism *Med Phys* **23** 307-316
- III. **Weber L**, Nilsson P, Ahnesjö A 1997 Build-up cap materials for measurement of photon head-scatter factors *Phys Med Biol* **42** 1875-1886
- IV. **Weber L**, Laursen F 2002 Dosimetric verification of modulated photon fields by means of compensators for a kernel model *Radiother Oncol* **62** 87-93
- V. **Weber L**, Nilsson P 2002 Verification of dose calculations with a clinical treatment planning system based on a point kernel dose engine *J Appl Clin Med Phys* **3** 73-87
- VI. **Weber L**, Ahnesjö A, Murman A, Saxner M, Thorslund I, Traneus E 2003 Beam modelling and verification of photon beam multi-source models. Manuscript

The original published articles have been reproduced with the permission of the following publishers.

Papers I and III have been reprinted with the permission of IoP Publishing Ltd.

Paper II has been reprinted with the permission of the American Association of Physicists in Medicine (AAPM)

Paper IV has been reprinted with the permission of Elsevier Science Inc.

Paper V has been reprinted with the permission of the American College of Medical Physics (ACMP)

The following preliminary reports have been presented throughout international scientific meetings:

The 3rd Biennial ESTRO Meeting on Physics for Clinical Radiotherapy, Gardone Riviera, Italy, October 8-11, 1995.

Weber L, Ahnesjö A, Nilsson P, Knöös T: Verification of a dynamic wedge implementation in a pencil beam based dose planning system. *Radiother Oncol* **37**, S96

The 17th Annual ESTRO Meeting, Edinburgh, Scotland. September 20-24, 1998.

Weber L, Ahnesjö A, Kivultjik I: Clinical accuracy of a pencil kernel model for wedge dose calculations *Radiother Oncol* **48**, S134

The 5th Biennial ESTRO Meeting on Physics for Clinical Radiotherapy, Göttingen, Germany. April 6-11, 1999.

Laursen F, Weber L: Evaluation of compensator filter calculations using a pencil kernel model *Radiother Oncol* **51**, S18

The 6th biennial ESTRO Meeting on Physics for Clinical Radiotherapy, Seville, Spain, September 17-22, 2001.

Weber L, Murman A, Ahnesjö A: Variability of clinical beam data for commissioning of treatment planning systems *Radiother Oncol* **61**, S88

Contents

1 Introduction	1
1.1 Accuracy requirements in external beam radiotherapy	1
1.2 Accuracy requirements in external beam treatment planning	2
1.3 Photon dose calculation algorithms	3
1.4 Model-based treatment planning	5
1.4.1 The photon multi-source model in Helax-TMS	5
1.5 Early QA of the photon dose calculation algorithms in the Helax-TMS treatment planning system	8
2 Aims of the current work	11
3 Data processing, implementation and validation	13
3.1 Quality assurance basics for the current work	13
3.2 Measurements as input to the multi-source model	14
3.2.1 Measurement variability of characterization data	16
3.2.2 Experimental determination of the head scatter factor	20
3.2.3 Treatment unit characterisation	23
3.3 Unmodulated fields	24
3.4 Modulated fields	25
3.4.1 Wedge-modulated beams	26
3.4.2 Collimator-modulated beams	27
3.4.3 Compensator modulated beams	28
3.5 Heterogeneities	29
3.6 Clinical examples calculated with Helax-TMS	29
4 Concluding remarks	35
5 Future directions	37
5.1 Experimental methods used for verification	37
5.2 Build-up region dose calculations	37
5.3 Standard data sets	38
5.4 Monte Carlo dose calculation techniques	38
Acknowledgements	39
References	41
Popular science summary (in Swedish)	51

1 Introduction

1.1 Accuracy requirements in external beam radiotherapy

Cancer is currently one of the major health threats in the world, with approximately 10.1 million new cases per year and 6.2 million deaths at the turn of the last millennium (Stewart and Kleihues 2003). The treatment of cancer diseases remains a challenge worldwide. In many cases, radiotherapy, alone or in combination with other modalities, e.g. surgery and/or chemotherapy, is the method of choice. The response of the tumour as well as the normal tissues can be described by what is referred to as a dose-response curve. The curve shape is usually sigmoid, i.e. most of the response occurs within a certain dose interval. The response depends on the type of radiation as well as on the biological characteristics of the tissue. These include the condition of the vascular system, the efficiency of the repair of radiation-induced damages, the delay in growth in different phases of the cell cycle and the capacity of the resting cells to enter the cell cycle, etc. (Steel 2002).

The normalised dose response gradient, γ , describes how large a change in response probability can be expected for a given relative increase in absorbed dose (Brahme 1984, Bentzen 2002),

$$\gamma = D \frac{dP}{dD}$$

where P denotes the response probability for a given dose, D .

Given the complex nature of cell populations there is a spread in γ and values up to 4 have been noted for injuries in some organs and as high as 9 for certain malignant tissues (Brahme 1988). The normalised dose gradient also includes dosimetric uncertainties and it is therefore crucial that radiotherapy can be administered as well as reported with a high degree of accuracy.

Several authors and organisations have developed requirements regarding the level of accuracy required in radiotherapy (Brahme 1984, Mijnheer *et al.* 1987, Van Dyk *et al.* 1993, Aaltonen *et al.* 1997). Most of these requirements originate from observations based on clinical studies (Brahme 1984, Mijnheer *et al.* 1987, Brahme 1988). Although they had different objectives, Brahme (1988) and Mijnheer *et al.* (1987) came to similar conclusions regarding the accuracy required for dose delivery.

Brahme (1988) argued that in order to ensure a reasonable probability of distinguishing the outcome of different treatment techniques or dose distributions with regard to tumour control probability, a relative standard deviation of less than $\pm 10\%$ is desirable. In a review article by Mijnheer *et al.* (1987) it was concluded, from a number of clinical observations, that an uncertainty in absorbed dose greater than 7% at the specification point could be subject to unforeseen normal tissue reactions. This 7% was taken as 2 SD, resulting in an overall uncertainty in absorbed dose of 3.5% (1 SD).

Radiotherapy is a complex mode of treatment and includes a number of steps that all introduce a certain level of uncertainty, which can ultimately contribute to the success or failure of the treatment. The dosimetry chain, for example, involves several steps towards obtaining a calibrated detector for determination of the absorbed dose to a reference point. This involves the secondary standard dosimetry laboratory (SSDL), which is usually the supplier of the calibration data for the reference detector at the hospital. The dosimetry of the SSDL is traceable back to a primary standard dosimetry laboratory (PSDL). In many cases, the SSDL calibration is transferred to a field instrument at the user organisation for redundancy purposes. The degree of complexity is increased when the calibration in water is transferred to relative dosimetry, used partly for accelerator QA and as input data for a TPS. The TPS in turn is used for the calculation of dose distributions in the patient for the planned treatment. In addition, the delivery of the TPS-calculated dose distribution is also subject to some degree of uncertainty including linear accelerator parameters, e.g. monitor stability, beam flatness, as well as the uncertainties in patient data and the subsequent set-up of the patient on the treatment table. The status in delivery and dosimetry have been summarised by e.g. Brahme (1988), Andreo (1990) and IAEA (2000). In addition to the delivery and dosimetry chain, the uncertainty in delineating the tumour and normal tissue also adds to treatment outcome.

1.2 Accuracy requirements in external beam treatment planning

The evolution of quality assurance, QA, in treatment planning has led to several publications on specific stages of the planning process and treatment techniques, e.g. van Bree *et al.* (1991), Essers *et al.* (1993) and Hurkmans (2001). The combined information from investigations such as these and similar ones has led to several QA recommendations for

TPSs. Regarding the issue of photon dose calculation algorithms for a TPS, a number of publications give recommendations regarding tests and accuracy limits, e.g. Van Dyk *et al.* (1993), Kutcher *et al.* (1994), Fraas *et al.* (1998) and Venselaar *et al.* (2001). One of the earlier publications that gave accuracy levels in external beam dose calculations was an ICRU report (ICRU 1976). Based on several clinical studies, ICRU recommended a minimum accuracy of $\pm 5\%$ in absorbed dose to a target volume (the figure was later interpreted as representing 2 SD (IAEA 2000)). This level was upheld and recommended in a subsequent report for the delivery of absorbed dose, but for computer-produced dose distributions in treatment planning a limit of $\pm 2\%$, or 2 mm in high dose gradient regions, was recommended (ICRU 1987).

While Brahme (1988) concluded that for treatment planning systems an uncertainty in the dose of 3 % (or 3 mm in position) is a realistic demand for photon beams, Ahnesjö and Aspradakis (1999) applied a different approach. The beam delivery accuracy (e.g. absorbed dose at the calibration point as well as at other points, treatment unit parameters and patient-related uncertainties) for currently employed techniques was found to be 4.1 % at best. This figure excludes any uncertainties in TPS dose calculations. In agreement with Brahme (1988) it was found that this would result in an overall uncertainty of 5.1 % (1 SD) provided that the TPS dose calculation accuracy could be maintained at 3 %, or better (see Table 2 in Ahnesjö and Aspradakis (1999)).

In a recent publication by Venselaar *et al.* (2001) a more detailed set of recommendations was given regarding TPS calculations based on dose and dose gradients. Different geometries were proposed and tolerances were recommended for these geometries. These limits are somewhat stricter than those recommended by previous authors, e.g. Van Dyk *et al.* (1993) and Fraas *et al.* (1998), but comparable to those given in SGSMP (1997).

1.3 Photon dose calculation algorithms

Dose calculations in external beam radiotherapy can be applied using a variety of techniques, starting with simple table-based systems to which most clinics have access. These are based on measurements in water with a reference geometry. Corrections are then made to the clinical situation using empirical methods, e.g. the tissue-phantom ratio (TPR),

the tissue-maximum ratio (TMR) or equivalent field size factors. A number of methods exist and the reader is referred to e.g. ICRU (1976), Johns and Cunningham (1983), Khan (1994) and Dutreix *et al.* (1997). These systems are still in use and their main objective is to allow for simple treatment techniques to be carried out, to check TPS generated charts, or to allow the use of beam qualities generally not implemented in a TPS, e.g. low and medium-energy X-rays. Other techniques involve isodose charts obtained in water for different field sizes superimposed on a coordinate system (usually a divergent fan line system). These have been combined manually in different beam arrangements and applied to a patient contour (ICRU 1987).

These simple library techniques were followed by implementation on computers when the possibility of using CT-based density information as the basis for the calculations became available. These first generations of computerized methods made use of tabulated data generated in water and stored in the TPS. To correct for the clinical situation, the beam is reconstituted using “Clarkson summation” (Cunningham 1972) or a similar technique. Correction for beam modifiers, if present, is also performed. The final step is to correct for patient outline and heterogeneities. These types of TPS are generally referred to as beam library systems. Following the classification by Mackie *et al.* (1996) this class of algorithms is referred to as correction-based algorithms.

To better comply with more stringent accuracy demands, a new generation of dose calculation algorithms evolved during the 1980s replacing the beam library models. These model-based algorithms, as they are generally known (Mackie *et al.* 1996), are associated with a more explicit modelling of the radiation transport. These new algorithms use convolution or superposition techniques based on dose deposition kernels. The kernels are usually precalculated using Monte Carlo techniques and contain the dose deposited by secondary charged particles around an interaction point, usually in water. Different investigators have given the kernels different names and may be referred to as a “dose spread array” (Mackie *et al.* 1985) or “differential pencil beam” (Mohan *et al.* 1986). The kernels used in the current work are called “point spread functions” by Ahnesjö *et al.* (1987) or “energy deposition kernel” by Ahnesjö (1989). Finally, the dose is given by a convolution/superposition of the kernel with the energy released from the photon energy fluence.

The energy deposition kernel, here called a pencil beam, was implemented in the investigated treatment planning system, Helax-TMS (Helax AB, Uppsala, Sweden), as described by Jung *et al.* (1997). This was later followed by an implementation of a point kernel method utilizing the collapsed cone technique (Ahnesjö 1989, Saxner and Ahnesjö 1998).

1.4 Model-based treatment planning

In contrast to the first generation of treatment planning systems which relied on dose data stored in beam libraries, these second-generation algorithms use principles based on physics. The “amount” of physics included depends on the model used and ultimately affects the accuracy that can be achieved. In the current work, a multi-source model has been investigated extensively using experimental methods.

1.4.1 The photon multi-source model in Helax-TMS

The model investigated in the Helax-TMS TPS is based on the assumption that different “sources” of radiation can be defined within the treatment head of an external beam treatment unit, e.g. a linear accelerator or cobalt unit. The primary photon energy fluence, Ψ_{prim} , constitutes after filtration the major part of the contribution to the dose and it originates at the point where the electron beam hits the target (Ahnesjö and Trepp 1991). In addition, a number of secondary sources exist within the treatment head. These are the flattening filter (Ahnesjö 1994), the collimators (Ahnesjö 1995) and any additional accessories in terms of wedges, block trays or compensators (Ahnesjö *et al.* 1995) that may have been chosen to modulate the beam

- flattening filter (Ψ_f),
- collimator edges (Ψ_c) and
- modulators (Ψ_m).

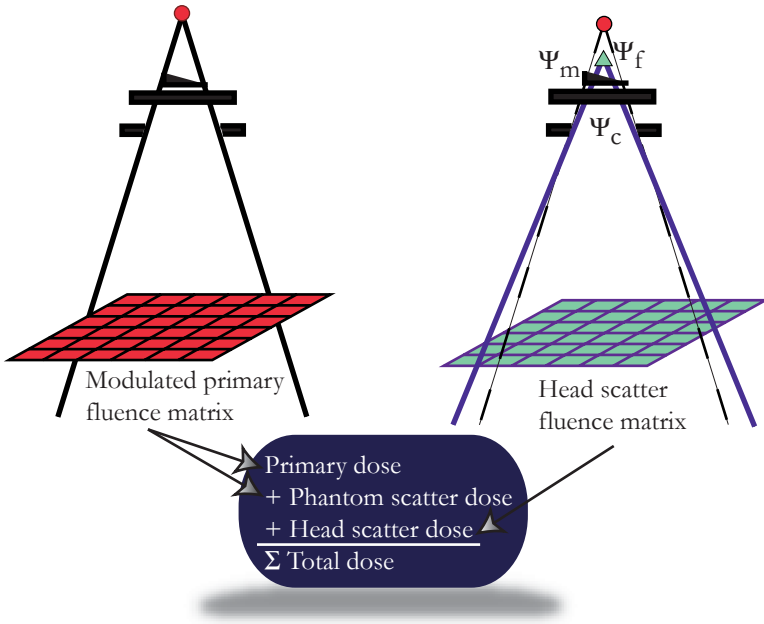


Figure 1. Energy fluence components within the treatment head. Auxiliary devices such as blocks, wedges, trays and compensators may also be present (not shown here).

The scattered radiation originating from these components is generally termed head scatter. The scatter component that contributes most to the absorbed dose in the patient is produced in the flattening filter (Chaney *et al.* 1994). As the other components contribute much less, the head-scattered photons are all assumed to radiate from the bottom level of the flattening filter for simplicity. In the current model, the amount of scatter generated in the primary collimator is included in the flattening filter scatter.

For each of the dose calculation points, the energy fluence from the primary and head scatter energy fluence are added to yield the total energy fluence. The primary energy fluence is factored into a reference level, Ψ_0 and a relative distribution, f . The dose per monitor unit, D/M , can then be expressed as (Ahnesjö *et al.* 1995):

$$\frac{D(\Psi_{\text{prim}} + \Psi_f + \Psi_c + \Psi_m)}{M} = \frac{\Psi_0}{M} d \left(f + \frac{\Psi_f + \Psi_c + \Psi_m}{\Psi_0} \right) \cdot \frac{1}{1 + M_b/M_0},$$

where Ψ_{prim} is the energy fluence from unscattered primary photons, Ψ_f is the scatter from the flattening filter (including the primary collimator), Ψ_c is the scatter contribution from collimators and block edges, Ψ_m is the scatter from auxiliary modulators such as wedges, trays or compensators and $1+M_b/M_0$ is a correction for backscatter from the upper side of the collimators into the monitor chamber. The data within the parentheses on the right-hand side of the equation, $d(\dots)$, are usually termed the dose engine and the parameters describing the dose engine, i.e. the point and pencil kernels, energy fluence distribution, energy spectrum, attenuation coefficients, head scatter parameters, charged particle parameters and beam source size, are derived during the treatment unit characterisation (TUC) process, and are unique for each beam quality. The dose deposition is dependent on the type of kernel implemented: the pencil or point kernel. Point kernels describe the energy deposition resulting from a forced interaction in a medium, in this case water. Through Monte Carlo simulations it is possible to pre-calculate the energy deposition in water and to separately “score” the different dose contributions: total, primary and scatter dose, by following a large number of photon histories. One of the disadvantages in using a point kernel method is that it is quite time consuming, as the calculations have to be performed in matrix geometries. To speed up the dose calculation time, the pencil kernel may be used instead. The pencil kernel can be seen as a pre-integration of the energy deposition in one of the dimensions, i.e. the depth dimension. Both types of kernels can be stored in a parameterised form (Ahnesjö 1989, Ahnesjö *et al.* 1992):

Pencil kernels:
$$\frac{p}{\rho}(r, z) = \frac{A_z e^{-a_z r} + B_z e^{-b_z r}}{r},$$

where A_z , a_z , B_z , b_z are stored for each depth, z , and radius, r , to the pencil axis (cylindrical co-ordinate system with origin at the phantom surface).

Point kernels:
$$h(r, \theta) = \frac{A_\theta e^{-a_\theta r} + B_\theta e^{-b_\theta r}}{r^2},$$

where A_θ , a_θ , B_θ , b_θ as function of the angle θ versus the impinging photon direction and r is the distance from the primary interaction point

(spherical co-ordinate system with origin at the primary photon first interaction point).

1.5 Early QA of the photon dose calculation algorithms in the Helax-TMS treatment planning system

Early QA work on the pencil beam dose calculation algorithm in the Helax-TMS TPS was carried out by Knöös *et al.* (1994) and Hurkmans *et al.* (1995, 1996). These investigations initially followed traditional lines and compared measured dose parameters with calculated data for the same geometry. Although belonging to a new class of TPSs, the technique used relied upon readily measurable entities that could be compared with calculated dose values, e.g. absorbed dose in water, as the kernel is difficult to measure directly using experimental techniques. Early results of dose calculations based on pencil kernel dose calculations indicated that model-based treatment planning could be at least as accurate as that achieved with older correction-based dose calculation algorithms. However, there remained some situations where the calculated dose occasionally was outside tolerance levels, see the summary in Table 1.

Table 1. Limitations found in early QA work. Reference details for tests 1 - 2 are available in Knöös *et al.* (1994) and for test 3 in Hurkmans *et al.* (1995).

Ref.	Test	Reason for deviation
1	Build up region	Exponential decay of the Gaussian kernel is too simple a model.
2	Output for larger field sizes (outside characterization domain)	The invariant pencil kernel results in too low a contribution from scatter generated in the patient.
3	Scattering volume effect	Pencil kernel integration for a kernel is done in a semi-infinite geometry and used in clinical situation where the finite patient geometry leads to an overestimation of scatter.

The investigation by Knöös *et al.* (1994) was performed using a simpler beam model (Helax-TMS version 2.8) than the one used throughout the current work. The conclusions drawn in their work are, however, generally valid. An exception is the result for wedged fields which uses a different approach as of Helax-TMS version 4.0 (Ahnesjö *et al.* 1995). The current dose calculation algorithm (Helax-TMS version 4.0 and higher) includes separation of the energy fluence into different sources of radiation and is referred to as a multi-source model. The work by Hurkmans *et al.* (1995, 1996) was performed using this multi-source model.

2 Aims of the current work

The first aim of the current work was to investigate the accuracy that can be achieved in a number of situations using a specific model-based TPS. The second aim was to experimentally study methods associated with the data collection for a model-based TPS and to investigate the variability of the basic input data, supplied for the model by several different departments. The particular TPS investigated (Helax-TMS) is a kernel-based TPS, initially released with only pencil kernels. At a later stage in the investigation, the TPS was refined so as to include the algorithm based on point kernels. The larger part of the investigation is hence focused on pencil kernel data.

The initial part of this study specifically involved validating the performance of Helax-TMS using the pencil kernel algorithm:

- lung tissue (**Paper I**),
- dynamically modulated beams (**Paper II**) and
- compensator-modulated beams (**Paper IV**),

and the point kernel algorithm in:

- a general investigation of the point kernel algorithm (**Paper V**).

The second part of this work involved the analysis of the underlying measurements used for model parameterization. The model used in the dose calculations is based on parameterised data derived during TUC, and is unique for each treatment unit and beam quality. The spread in dose calculations, for the model generated from the measured data, based on commissioning data from several users, was investigated as well as the underlying measurement sets used for the TUC process. The second part of this study was thus focussed on the implementation data in:

- an experimental study of build-up caps (**Paper III**), and
- an evaluation of the data implementation results (**Paper VI**).

Publications related to the pencil kernel algorithm implemented are found in **Papers I, II, IV and VI** while **Papers V and VI** are associated with the point kernel algorithm implemented. **Paper III**, finally, is entirely related to an experimental study.

3 Data processing, implementation and validation

3.1 Quality assurance basics for the current work

QA procedures for treatment planning systems have been described in a number of publications e.g. ICRU (1987), Van Dyk *et al.* (1993) and Kutcher *et al.* (1994). These publications include dosimetric as well as non-dosimetric issues, e.g. aspects related to the representation of the patient, in- and output peripherals, hardware testing, etc. In a recent publication by the American Association of Physicists in Medicine, AAPM, (Fraass *et al.* 1998) a formal set of recommendations was given. Most countries have hitherto, however, not adopted any formal regulations. It should also be taken into context that publications such as those referred to above have been produced at a time when beam library systems prevailed.

Although the introduction of kernel-based treatment planning systems resulted in a completely different approach to dose calculations, experimental QA methods have not changed. The primary components in the kernel-based treatment planning systems, i.e. energy fluence components, energy spectrum and dose deposition kernels, are difficult to determine and validate experimentally. Kapatoes *et al.* (1999, 2001) and O'Connor and Malone (1989), as well as Ceberg *et al.* (1996) and Storchi (1999) have, for example, made attempts to indirectly determine the incident energy fluence and the energy deposition kernel. While being conceptually important quantities, they are still difficult to use in practical comparisons.

*The approach employed in the current investigation was therefore to use readily measurable data such as dose in water. This has the advantage that data can be compared with **i**) existing recommendations, **ii**) measurements by other investigators, **iii**) data from treatment planning systems based on different algorithms.*

Output measurements in water, i.e. absorbed dose per monitor unit, have been made using standard Baldwin-Farmer type ionisation chambers. These output measurements were performed using an isocentric set-up in water with a source-surface distance (SSD) of 95 cm or 90 cm depending on the beam quality studied. A five-cm margin of phantom material was always present in order to maintain the scattering properties (IAEA 2000). Line doses (dose along the line connecting two

arbitrary points in space), i.e. dose profiles usually at a fixed depth, and depth doses, have been measured in water in a commercially available water phantom. Ionisation chambers have been used for depth doses and silicon diodes have been used for profiles. In the study described in **Paper II** a diode array detector (Leavitt and Larsson 1993) was used for the measurement of profiles. The exception to the above was data acquired in the heterogeneous geometry studies presented in **Papers I** and **V**. This geometry was simulated using Monte Carlo techniques.

In the early investigations (**Papers I** and **III**) a standard normalisation relative to a point at 5 or 10 cm depth, depending on beam quality, was used. When a more general head scatter model was introduced in the TPS, it also allowed for the calculation of the different components in the dose calculation. A more suitable means of normalisation then became the so-called output factor normalisation, d_i^{OFN} ,

$$d_i^{OFN} = \frac{(D(\mathbf{r})/M)}{(D/M)_{calib}}$$

where D/M is the dose per monitor unit for an arbitrary geometry at a point \mathbf{r} and for the calibration geometry, respectively. This method of normalisation preserves the absolute dose characteristics of the radiation field as it is linked to the absolute dose through a given calibration geometry of the TPS for each beam quality.

3.2 Measurements as input for the multi-source model

Treatment unit characterisation is designed to be general enough to be applicable to all medical linear accelerators commercially available, as well as to most Co-60 treatment units. The workflow to derive model parameters for photons during TUC is described in **Paper VI**. Figure 2 on next page shows the TUC flow sheet.

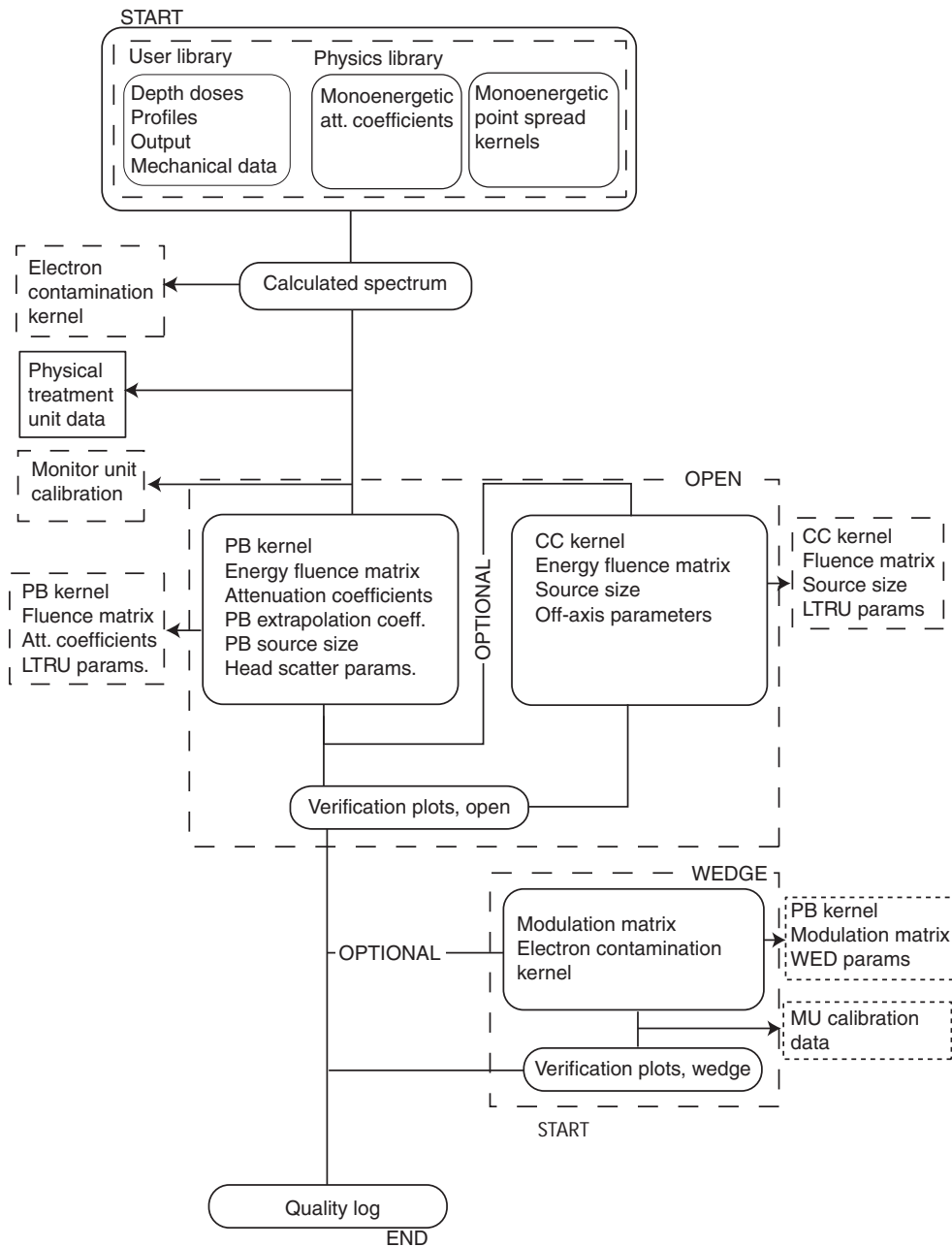


Figure 2. Flow chart for treatment unit characterization. The output is subdivided into three groups: i) physical treatment unit data (PTRU), e.g. distances, scales and angular information – box with solid line, ii) logical treatment unit data (LTRU), e.g. beam quality related parameters – boxes with long dashed lines, iii) wedge data (WED), e.g. wedge related parameters – boxes with short dashed lines.

The program is executed under the operating system VMS and data are read into the program by reading a purposely structured file. This file contains mechanical data, beam quality data, administrative data as well as dosimetric data. These dosimetric data are the results of measurements performed at the time of commissioning the accelerator for the TPS. The file generated prior to running the characterisation step serves as a “receipt” of the input and can also be reused at a later stage. From a QA, as well as regulatory, point of view this is a crucial step.

The output consists of structured data in several files, mainly ASCII files but some binary files containing the open energy fluence matrix and the wedge modulation matrices (if present) also exist. At the top level the physical treatment unit, “PTRU” containing parameters describing the treatment unit and auxiliary devices can be found. At the next level down is a logical treatment unit, “LTRU”, and this is associated with dosimetric parameters for each open beam quality. Just as with a real medical accelerator, there may be one or more LTRU units. This is the minimum configuration for performing dose calculations in the TPS. If wedge data exist, one or several wedges can be associated with each logical treatment unit. These wedges can be mechanical wedges, motorised or fixed wedges, as well as “soft” wedges, e.g. VW[®], DW[™], EDW^{™*}.

Although the multi-source model is based on physical principles it relies heavily on measured data to derive the parameters used in the model. Current state-of-the-art algorithms all use this approach and the first generation of clinical Monte Carlo algorithms also uses this approach as it is difficult to obtain the necessary detailed knowledge of the treatment head and beam optics for all accelerators. Even full Monte Carlo simulations still rely on limited measurement sets to determine the correctness of the accelerator model simulated in the Monte Carlo system. Hence, measurements will probably still be an integral part of any treatment planning system of the future.

3.2.1 Measurement variability of characterization data

A number of measurements are used as input to the treatment unit characterisation and Table 1 in **Paper VI** summarises these. A large number

* DW and EDW are trademarks of Varian Medical Systems, Inc and VW is a registered trademark of Siemens Medical Systems, Inc

of data sets submitted to the vendor for treatment unit characterisation have been evaluated in terms of variability for the same accelerator type and nominal energy. Emphasis has been placed on the newer generation of accelerators, as these are naturally the most abundant, as well as having the advantage that through computer control of the accelerator they should be less susceptible to instabilities in the beam optics. The focus on the data presented here (Weber *et al.* 2001) is for 18 MV photons from a Varian Clinac 2100^{®*} accelerator, but similar results can be found for other treatment units. No information is available regarding the experimental equipment used but it is assumed that each clinic uses reliable equipment. The recommended approach is, however, to use small volume ionisation chambers for depth doses and silicon diodes for profiles. Output should be measured using Baldwin-Farmer type ionisation chambers. The data were evaluated by generating the mean value of the samples available. The spread in data is expressed as 1 SD.

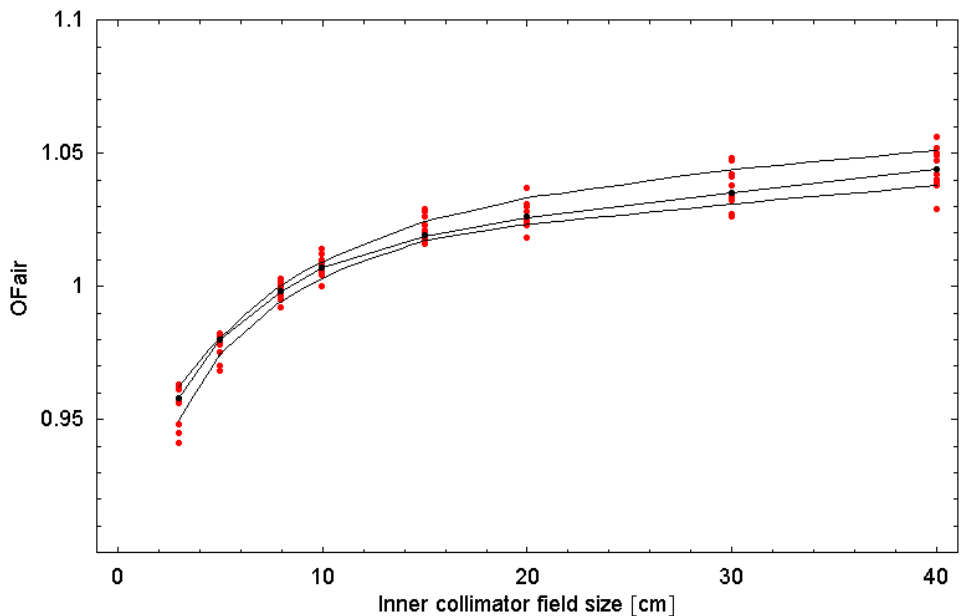


Figure 3. Output measurements in air at the isocentre for rectangular open fields used for input for the derivation of head scatter parameters. The lower collimator is fixed at 40 cm. Data are normalised to the 10 cm × 10 cm open field. Solid lines denote the mean value ± 1 SD, dots are measurements.

* Clinac is a registered trademark of Varian Medical Systems, Inc.

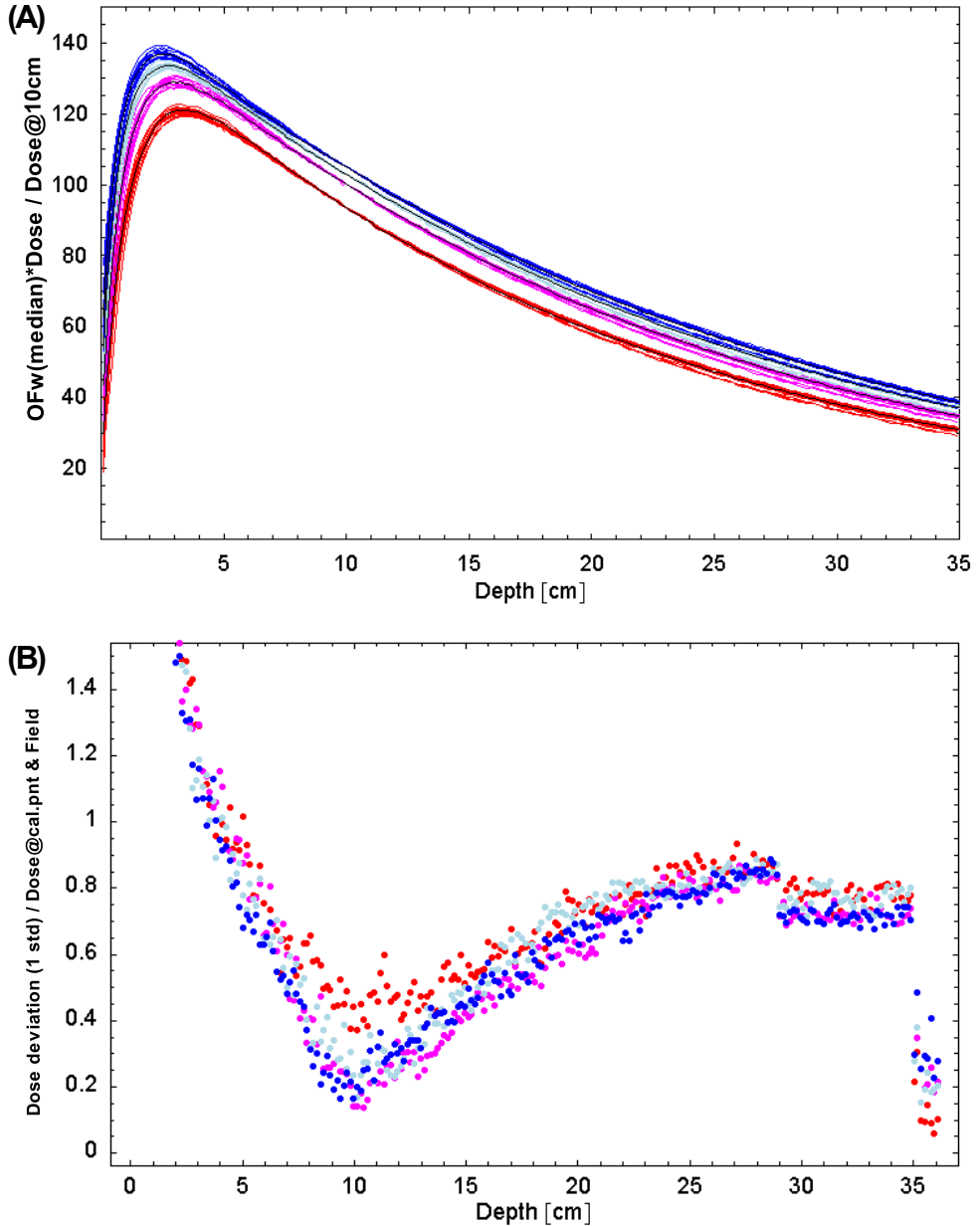


Figure 4. Square open field depth dose measurements in water (A) and mean value (B). Field sizes as used for the determination of point and pencil kernels, as well as charged particle contamination kernels, blue = 20 cm × 20 cm, cyan = 15 cm × 15 cm, magenta = 10 cm × 10 cm, red = 5 cm × 5 cm. Data normalised to 10 cm depth and SSD=90 cm. Black lines = mean of all measurements.

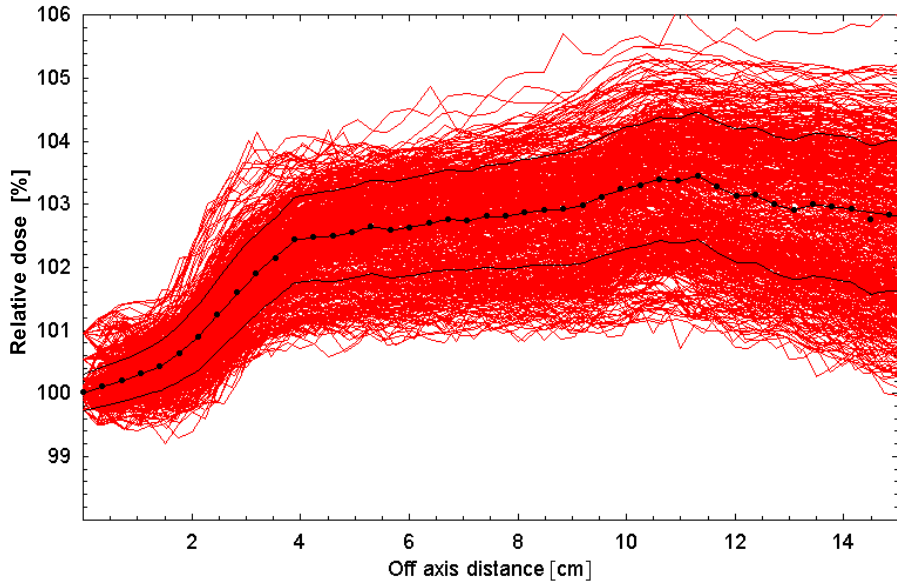


Figure 5. Part of open star profiles from isocentre out to a distance of 15 cm. Red lines – all measurements, black lines – median of all measurements ± 1 SD.

As can be seen in Figure 3 - Figure 5 the variation between different accelerators of the same model is quite small and in general amounts to less than 2 %, including measurement uncertainties. The highest deviations are found in regions where the choice and use of experimental equipment is crucial such as in the build-up region. Using an ionisation chamber will give quite different results from silicon diodes due to large differences in spatial resolution. The choice of build-up cap is also crucial in determining the output factors in air and will be further discussed in section 3.2.2 below.

As the variation is quite small, a standard set of data could be introduced as an alternative to a full commissioning procedure. Data sets like these could also facilitate the commissioning of the TPS where users do not have the equipment necessary to measure some of the parameters, for example, scanning phantoms large enough to measure the mandatory so-called star profiles (**Paper VI**). Such an approach could also lead to faster commissioning of new versions of a TPS when common data can be shared between user groups.

3.2.2 Experimental determination of the head scatter factor

Two major methods exist for measuring output factors in air, i.e. the head scatter factor. One is the use of high-density build-up caps (Kase and Svensson 1986, Spicka *et al.* 1988, Frye *et al.* 1995) and the second is the use of mini-phantoms (van Gasteren *et al.* 1991, Tatcher and Bjarngard 1993, Dutreix *et al.* 1997). Both techniques allow for measurements beyond the depth of contaminant charged particles and measurements under electronic equilibrium. The small dimensions also allow for measurements in beams with small apertures.

An extensive investigation of the technique for in-air measurements has been made (**Paper III**). Some commonly available materials, i.e. polystyrene, graphite, brass and lead, were compared in terms of relative output for a set of square fields. The basic wall thickness recommendation of the TPS vendor for collecting beam data was followed, i.e. to have a thickness (in g/cm^3) of $U/3$, where U is the nominal accelerator potential in MV. This thickness is chosen to eliminate contaminating charged particles emanating from the treatment head. Similar results were obtained in all cases, although the build-up caps made of high-density materials showed minor differences from the low-density materials when the nominal energy was increased. The major advantage of using the high-density caps is the smaller dimensions allowing for measurements in fields with small apertures. This is crucial, as it is in this field size range the largest changes in output occur due to the changes in flattening filter scatter. This happens as a consequence of the collimators obscuring the view from the measurement point of view. Once the complete flattening filter is visible, only the collimator scatter and monitor chamber backscatter add to the reading. The high density build-up caps therefore allows for a sufficient number of measurement points to adequately determine the head scatter parameters. High density build-up caps also avoids using measurement techniques at extended SSD and converting the readings to isocentre distance (Khan *et al.* 1996).

A frequently used measurement technique is to place the ionisation chamber parallel to the radiation beam. Although the exact location of the measurement point is not well known, the uncertainty introduced is very small and is minimised by the use of a normalisation towards a reference field, usually $10\text{ cm} \times 10\text{ cm}$. The recommended wall thickness agrees with recommendations given by Allen Li *et al.* (1995) for achieving lateral electron equilibrium. In the example below, a graphite phantom

was used, similar to the mini-phantom but with dimensions large enough to achieve lateral electron equilibrium for graphite at the highest energy available, 18 MV. The thickness in the incident direction is varied by

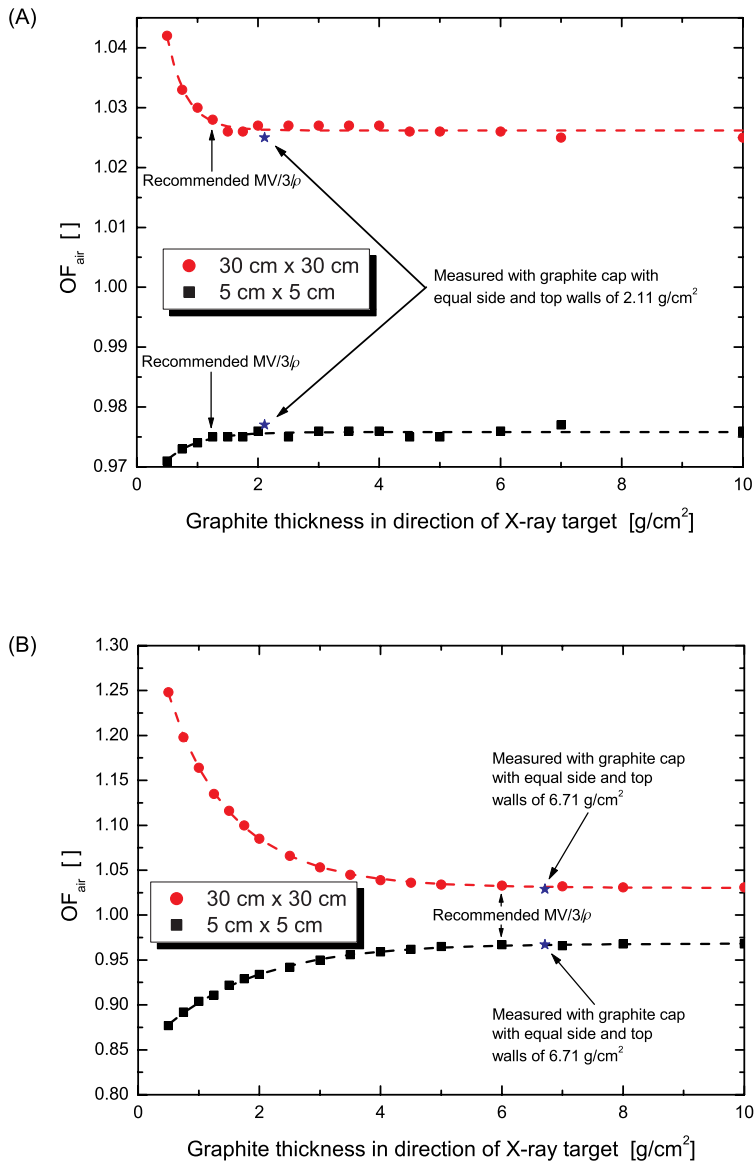


Figure 6. Measured results for (A), 4 MV and (B), 18 MV photons with phantom material graphite, $\rho = 1.863 g/cm^3$ and constant wall thickness = $2.142 g/cm^2$. The dashed line indicates a polynomial fit to the measured data.

adding disks of the same outer dimensions as the main body, while the lateral dimensions are kept fixed according to the recommendation of Allen Li (1995) for the materials graphite and brass.

It can be observed that the recommended thickness is sufficient with this measurement technique, although the combination of low energy and low density falls on the part of the curve where the signal is not completely saturated. This may be of minor importance as measurements under electronic disequilibrium should be possible (Allen Li *et al.* 1995).



Figure 7. Build-up cap and coaxial phantom used for the measurement of output factors in air. Back left, brass build up cap for BF chambers. Middle front: mini phantom equivalent to the graphite mini-phantom on the right, including bits to surround the stem. Also shown are the disks used to vary the thickness in the beam direction.

The small-volume ionisation chamber used, RK 83-05* (Johansson *et al.* 1987), was extremely sensitive to the phantom design around the stem. It was found to be necessary to surround the stem with phantom material and avoid air channels along the chamber. The design can be seen in Figure 7.

3.2.3 Treatment unit characterisation

Paper VI deals with the results of the processing of a large number of data sets for a variety of available treatment units processed during a certain time frame. TUC is based on a sub-set of an established set of measurements that also includes additional scans for verification purposes. Calculated dose data in water have been compared for the full measurement set. It is shown that the dose results using the calculated model parameters are within 1.0 % of the measurements for the open fields available for both algorithms, point and pencil kernels. These results were obtained using automated routines for the model parameters during data processing. The variations seen here are generally small and randomly distributed for both the point and pencil kernel models, see Figure 8.

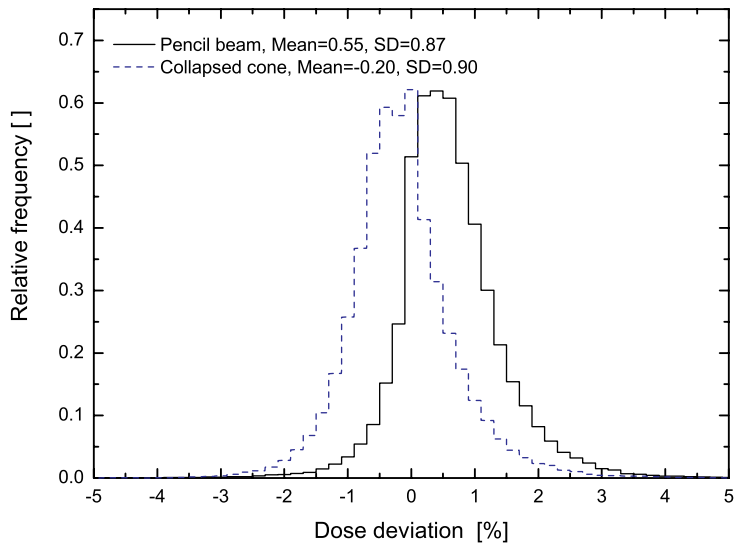


Figure 8. Point and pencil kernel dose deviations in percent of the calibration dose for open beams in the range 4 – 25 MV.

*Scanditronix-Wellhöfer AB, Uppsala, Sweden.

Approximately 80 % of the data available for modelling shows deviations of less than 2 % of the calibration dose. The deviation increases when the wedge is introduced during characterization. Treatment units with a 60° wedge show error levels of 3.0 % and 4.2 % (1 SD) for the largest field, for the point kernel and pencil kernel algorithm, respectively.

3.3 Unmodulated fields

The pencil kernel is a descendent of the more general point kernel where the monoenergetic kernel has been integrated along the depth axis to save time during dose calculations. As was shown by Knöös *et al.* (1995) and in **Paper I** this leads to some limitations. The first limitation is related to larger field sizes. As the pencil beam kernel is energy invariant, it leads to underestimation of the output with increasing field sizes. This is mostly noticeable outside the characterisation domain in this model, i.e. field sizes larger than 20 cm × 20 cm. As the pencil kernel is spatially invariant, scatter contribution will be overestimated centrally where the photon energy in the real beam is higher. Analogously, underestimation of the scatter will occur from peripheral regions when the photon energy in the real beam is lower (due to off-axis softening) compared with the calculated pencil kernel dose.

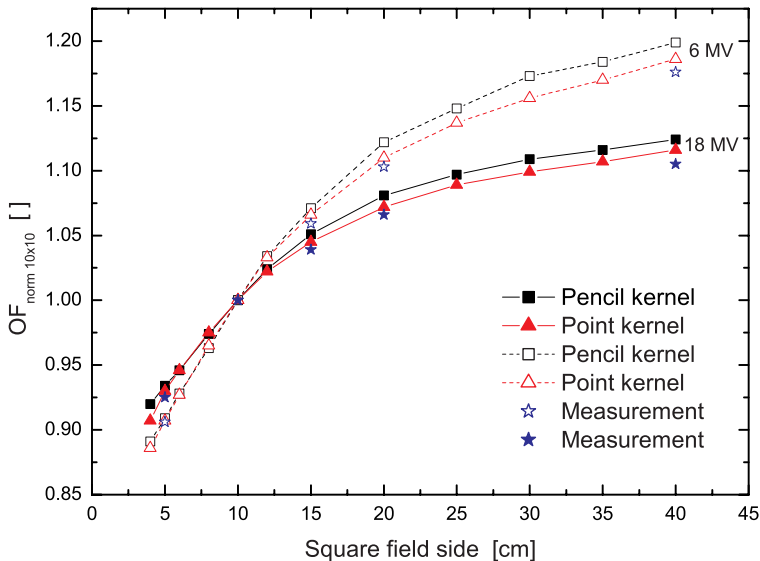


Figure 9. Output in water for 6 and 18 MV open fields for pencil and point kernels.

From the single test of the treatment unit used in Figure 9 above it is evident that the output calculations outside the characterisation domain are better handled by the point kernel algorithm where the effect of off-axis softening is included.

A second weak point is the dose calculation in the build-up region. When the primary photons traverse the treatment head they interact with, for example flattening filter, collimators, wedges and blocks used for field shaping, and produce secondary charged particles. This results in a complex scenario dependent on the treatment unit design in combination with the planned beam set-up (Sjögren 2001). In the Helax-TMS TPS, the primary kernel is based on Monte Carlo simulated particle transport in an irradiated phantom and does not take into account the effects of contaminant particles. The lateral distribution of charged particle contamination is modelled as a Gaussian kernel together with a longitudinal exponential decrease, taken as the difference between the pure Monte Carlo simulated kernel and the measurements for the same fields. These kernels are unique to each beam quality as well as each mechanical wedge and each modulator material. The model is described in the work by Ahnesjö and Andreo (1989) and Ahnesjö *et al.* (1992).

While this model may give acceptable results for the simplest cases it may give less satisfactory results in other situations, specifically at high energies (Knöös *et al.* 1994). This behaviour has also been confirmed by Spezi *et al.* (2001). Hence, use of *in vivo* dosimetry must be based on procedures where the electron contamination level is low enough not to jeopardize the calculated results. The use of the TPS calibration geometry involving the dose maximum, as is still frequently done where the TG-21 dosimetry protocol (AAPM 1983) prevails, should therefore be avoided. As shown in **Paper VI**, however, the accuracy for unmodulated beams is satisfactory in the majority of situations.

3.4 Modulated fields

The quantity most suitable for describing the energy content of the radiation emanating from the treatment head is the energy fluence. The energy fluence approach allows for the incorporation of devices commonly used in clinical routine, e.g. blocks, wedges or modulators. Combinations of these may also occur frequently in clinical practice. The primary beam energy fluence may be expressed at a reference level, usually for the maximum field size available at a reference distance.

In addition, the effects of the treatment head acting as a source of scattered radiation as well as the secondary effects of the modulators are incorporated into the two energy fluence matrices (Saxner and Ahnesjö 1998).

The modulation of the primary energy fluence for wedges and compensators in this study follows the work of Ahnesjö *et al.* (1995) and includes effects on the primary transmission as well as effects on beam quality caused by the attenuator. Modulation generated by the movement of jaws (or multi-leaf movements) is handled according to the description in **Paper II**.

3.4.1 Wedge-modulated beams

Modulated fields can be created by the introduction of mechanical wedges (fixed-angle wedges or motorized wedges) or compensators (see section 3.4.3). In both cases careful modelling of the effects introduced by the modulator must be performed. Apart from the attenuation of the primary fluence, secondary effects include beam hardening introduced by the attenuator, as well as the additional scatter generated in the attenuator. These effects must be taken into consideration. A model for this has been presented by Ahnesjö *et al.* (1995).

As can be seen in **Paper VI**, the modelling of mechanical wedges results in larger deviations than those found in unmodulated radiation fields. To some extent this may be attributed to the more complex modelling of the phenomena introduced by the modulator (Ahnesjö *et al.* 1995). Another source of uncertainty is the experimental situation where large dose gradients across the beam require a higher degree of experimental accuracy. For pencil beams there is no predominance of any particular type of deviation of the profiles, i.e. too flat, too steep, too concave or too convex, there is a tendency for the point kernel algorithm to create dose profiles in the wedged direction that are too steep. Currently, the model uses the modulation from the pencil beam modulation generation for both kernel types. This may be justified by the fact that modulation is independent of the type of kernel used as it is related to the attenuation of the energy fluence. A higher degree of accuracy could be achieved if point kernels were used to derive the modulation matrix for wedges.

3.4.2 Collimator-modulated beams

In many clinical situations there is a need to change the energy fluence across the beam. Changes in the energy fluence may be necessary in order to tailor the dose distribution to suit a particular physical or biological objective function. In the simplest case, several beams can be added manually to obtain a suitable dose distribution. This can be achieved by several methods, the simplest of which is to incorporate a physical wedge. Once computers were introduced as a means of controlling linear accelerators, more degrees of freedom were available to control the linear accelerator. One of the earlier inventions was to generate wedge-shaped dose distributions as a replacement for mechanical wedges (Kijewski *et al.* 1978, Levene *et al.* 1978). Sweeping one of the collimators across the aperture while the radiation beam is on, and keeping the remaining collimators fixed, generates the wedge shape. This method has some advantages over the physical wedges. In terms of handling, there is no lifting of heavy wedges involved, and the absence of the physical wedges decreases the dose from induced activity to the staff handling them. **Paper II** describes the implementation of dynamically collimated beams and the results in a variety of situations for “soft” wedges. Although the concept of modulation discussed here specifically deals with “dynamic” wedges, e.g. DWTM, EDWTM and VW[®], it is general enough and equally well suited for handling of multi-leaf modulation.

From a treatment planning point of view the handling of soft wedges is in fact easier than conventional wedges as no beam hardening effects are involved (Shih *et al.* 2001). Also, the additional scatter introduced by physical wedges need not to be addressed. Dose calculation involves the energy fluence and modulates it according to the so-called segmented treatment table (STT) of the accelerator. The STT gives the cumulative number of monitor units at a given position for the wedged field. The only task remaining is to calculate the modulation based on the STT. The model used here uses the cumulative monitor units for the field (**Paper II**).

One of their main advantages over physical wedges is that no extra measurements are required to model soft wedges. The specification of the jaw movement is required and this is given by the manufacturer.

3.4.3 Compensator modulated beams

For modulators with arbitrary shapes, i.e. compensators, a method was developed that would allow for large amounts of dosimetric information to be collected while keeping the number of compensators as small as possible (**Paper IV**). The method used was to generate a compensator for a large field size. This compensator can then be used for measurements in different types of fields; output measurements as well as depth doses and profiles for other field sizes or asymmetric fields. While this may not give the desired compensation for the particular field of interest, it is of minor importance as the aim is to evaluate the accuracy of the dose calculation algorithm. **Paper IV** shows the agreement between measurements and calculations to be within 3 % inside the field, but there are cases in the penumbra region where this is increased to 4 % or 2 mm positional error. It is obvious that careful implementation design in the TPS is also required. In the current implementation, Helax-TMS version 4.0 and higher, the modulator implementation replaces the standard set of parameters describing the beam quality. This gives a better description of the modulated beam but it compromises the accuracy of the non-modulated beam by using the parameterisation of the modulated beam. Since the majority of treatments (depending on departmental practice) include open beams, the gain in accuracy for modulated beams actually compromises the overall accuracy.

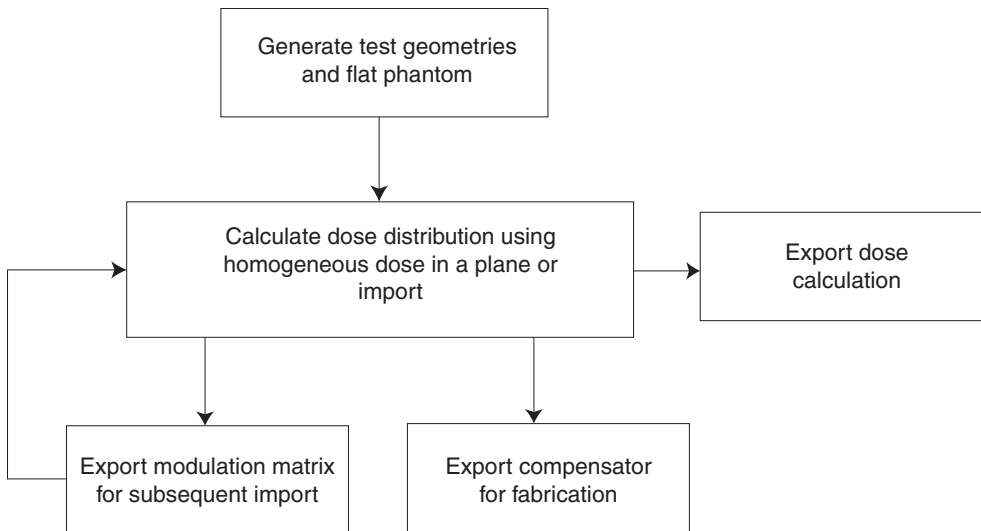


Figure 10. Flow sheet for generating the compensators as used in **Paper IV**.

As has been noted by other investigators (Basran *et al.* 1998, Spezi *et al.* 2001) the uniformity in an arbitrarily chosen plane is less satisfactory. This was considered to be an implementation problem in the TPS and could certainly pose a problem in a clinical planning situation. An alternative method of generating the desired dose profile for the plane was also suggested by Spezi *et al.* (2001). In the context of dose calculations this will, however, not influence the results.

3.5 Heterogeneities

Dose calculations in or close to heterogeneities have, in many cases, been associated with large errors as reported in several publications (el-Khatib and Battista 1986, Arnfield *et al.* 2000, Jeraj *et al.* 2002). The pencil kernel algorithm is no exception to this phenomenon, as shown in **Paper I** and elsewhere (Lewis *et al.* 2000, Blomquist *et al.* 2002) where large errors, increasing with photon energy, are present. The basic approach for the pencil kernel algorithm in heterogeneous media is to calculate a correction to the primary dose using an equivalent path length method. The scatter dose in turn uses a convolution determined correction factor depending on the depth in the patient or phantom assuming slab-like heterogeneities for ray-tracing along the beam paths. This approach neglects lateral effects and yields less satisfactory results when lateral charged particle equilibrium does not prevail.

The longer range of the secondary electrons in the low-density region is well modelled by the point kernel algorithm, see Figure 11 on next page, while this is not seen at all in the pencil beam algorithm. Many of the physical phenomena lost in the pencil kernel dose calculation, e.g. penumbra widening, re-build-up of dose, are more correctly modelled by the collapsed cone algorithm.

3.6 Clinical examples calculated with Helax-TMS

The current investigation, with its two main dose calculation algorithms, also has clinical impact. The pencil kernel appears to be best suited in regions where homogeneous volumes prevail. This would render the pencil kernel suitable mainly for planning target volumes (PTV) located in the trunk as well as in the skull (where no air cavities are present). The point kernel dose calculations are more demanding, as the complete CT volume must be calculated. The point kernel algorithm is therefore

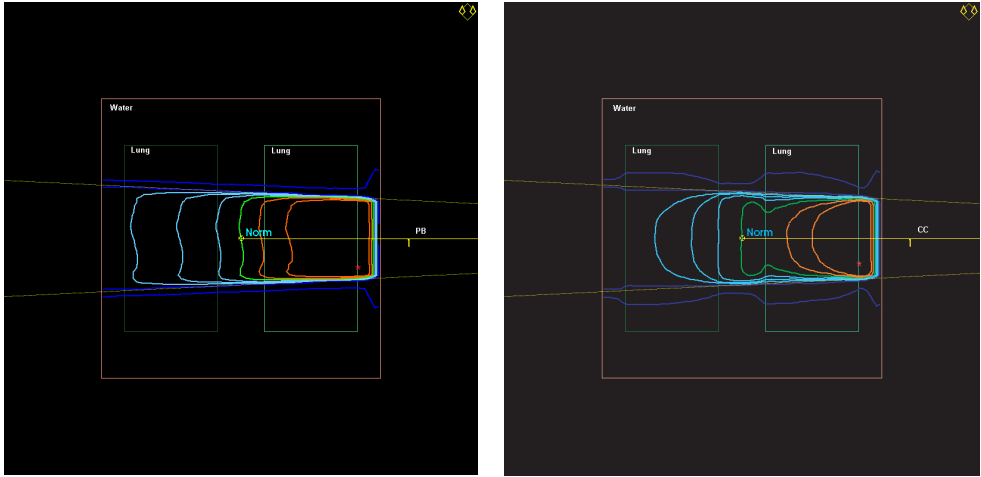


Figure 11. Dose distributions in a phantom geometry having a low-density region for 18 MV photons using a pencil (left panel) and a point kernel (right panel). Isodose levels displayed are 10, 50, 70, 80, 90, 100, 110 and 120 %.

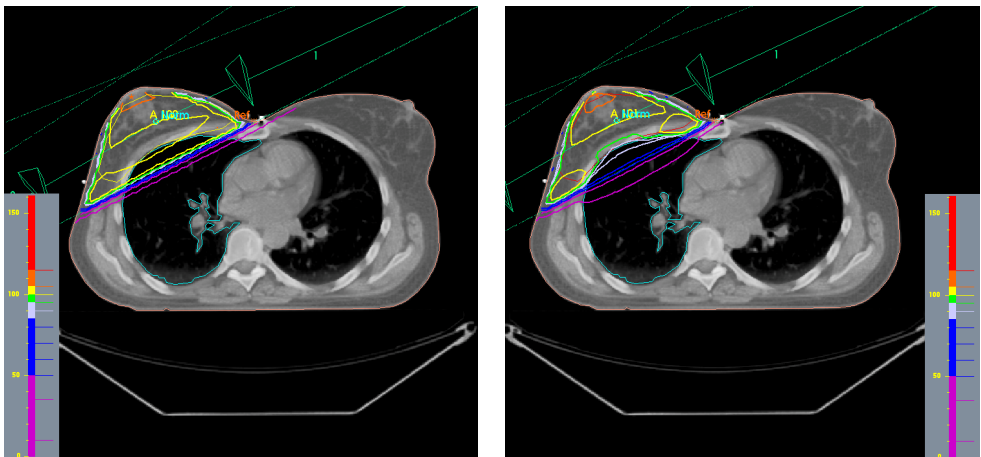


Figure 12. Dose distribution for pencil and point kernel calculations for a typical breast case using 6 MV photons. To the left, pencil kernel, and to the right, point kernel. Isodoses of 10, 30, 50, 70, 90, 93, 95, 100, 105 and 110 % are shown.

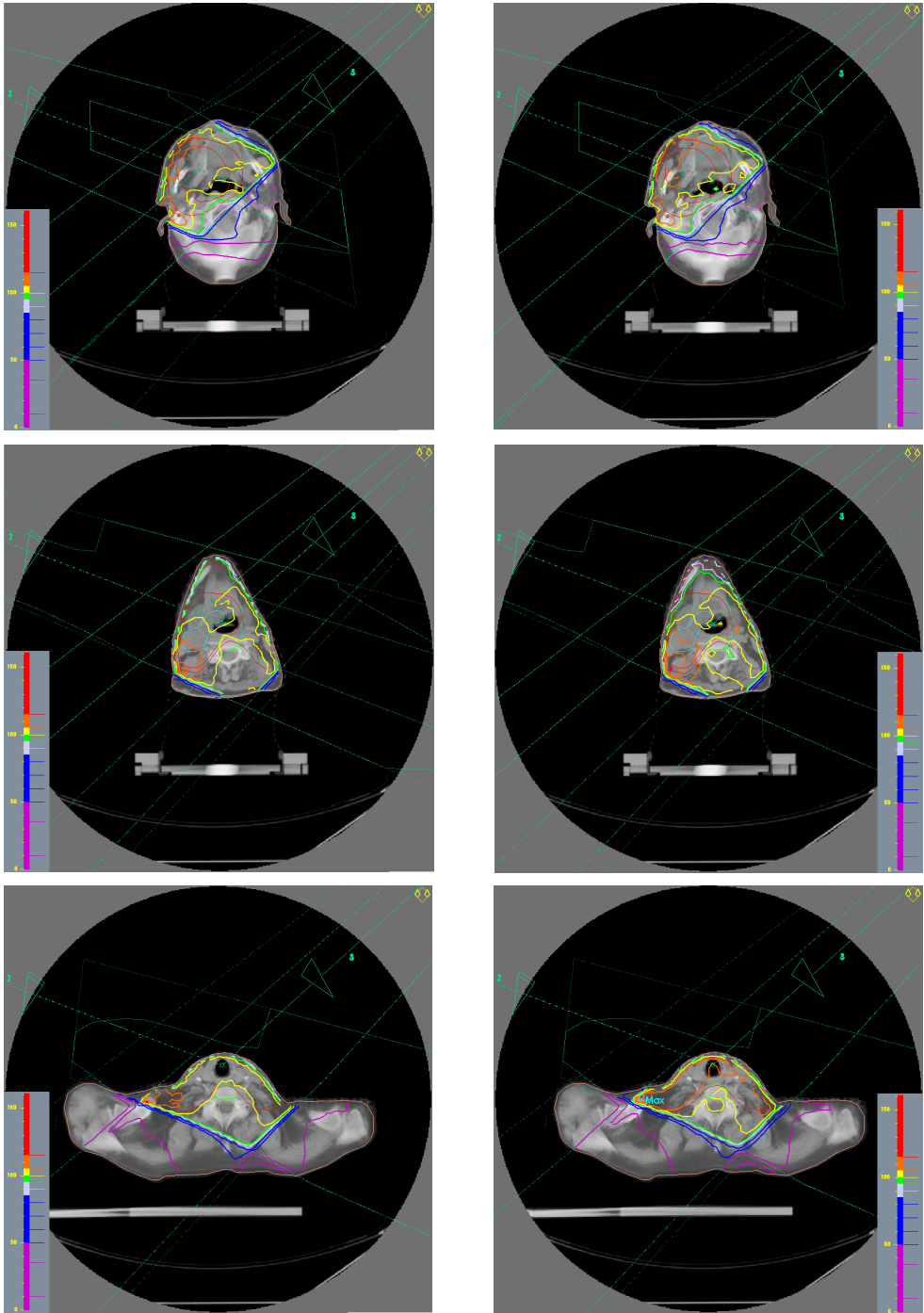


Figure 13. Dose distribution for pencil and point kernel calculations in the head & neck region using 6 MV photons. To the left, pencil kernel and to the right, point kernel. Isodoses of 10, 30, 50, 70, 90, 93, 95, 100, 105 and 110 % are shown.

best suited for regions including air cavities, where the largest differences between the two calculation modes exist. This includes the thorax and the head & neck region. Treatment planning for breast cancer patients is also included in this group as the patient scattering properties are poorly accounted for by the pencil kernel model.

The results obtained in the current investigation of phantom geometries also have several clinical implications. Illustrations of the results using the two dose calculation algorithms for a clinical PTV drawn in the head & neck region and a breast case are shown in Figure 12 and in Figure 13.

The dose volume histogram, DVH, in Figure 14 shows the difference between the two calculation models. The higher dose for the point kernel can be attributed to the way in which the PTV is drawn. Delineation of the PTV does not exclude the regions in the PTV containing air. The effect will be a higher dose inside the PTV due to the air cavities present. Although not relevant, since the dose deposition takes place in air, the dose will still be seen in the DVH and could lead to incorrect conclusions.

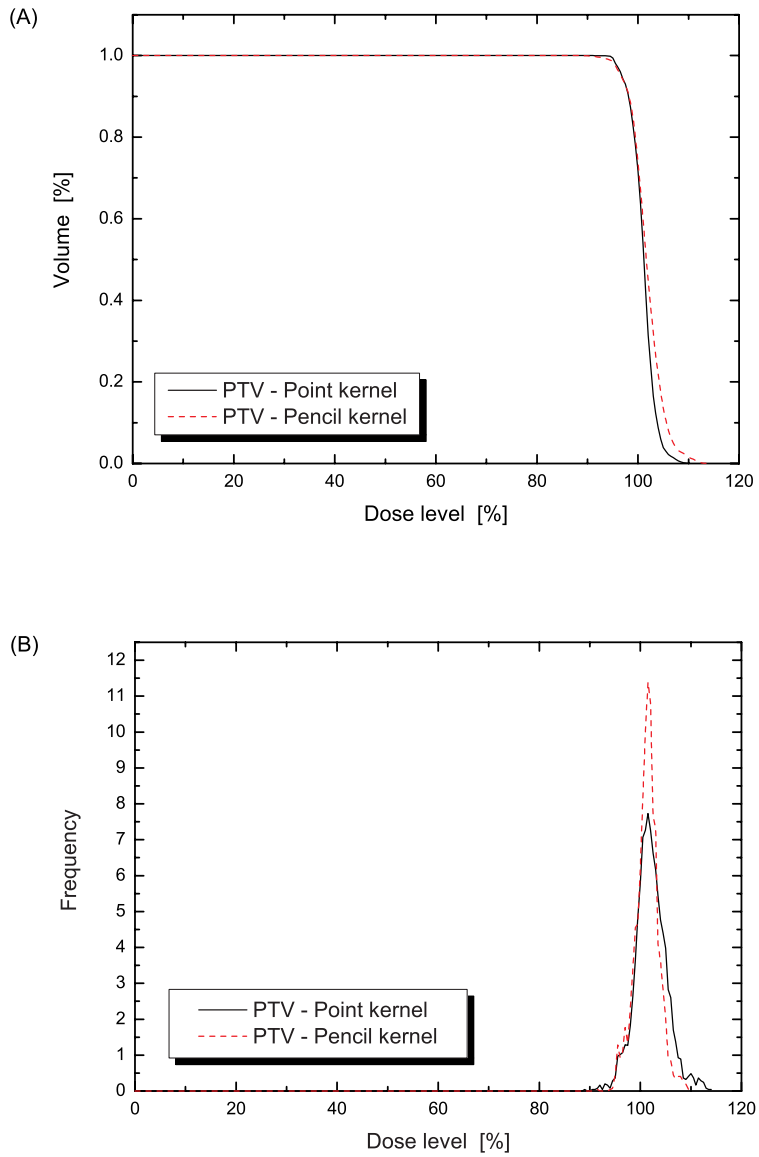


Figure 14. DVH, cumulative (A) and frequency (B), for the pencil and point kernel calculations in the head & neck region using 6 MV photons.

4 Concluding remarks

Commissioning of treatment planning systems is a time-consuming and complicated task. In addition to this, information regarding the algorithms must be gathered from the manufacturer as well as from the scientific literature. A number of measurements must be performed according to specified criteria in order to be able to perform treatment planning. Sometimes this also requires specialised measurement equipment (**Paper III**). These measurements are converted to model parameters in the case of model-based treatment planning systems (**Paper VI**). In this study the spread in the modelled data for some contemporary medical electron accelerators was analysed (**Paper VI**). For open beams the agreement between measured and calculated data was excellent. When wedges were introduced to modulate the beam the accuracy gradually decreased with increasing wedge angle.

It was found that reliable treatment planning could be performed, specifically using the point kernel algorithm for a wide range of clinical static and modulated beams. In the case of the pencil kernel algorithm some limitations were found (Knöös *et al.* 1995) and **Paper I**). These pertain mainly to the output for field sizes outside the characterisation domain, the build-up region and when heterogeneities are present (**Paper I**). The dose calculation algorithm using point kernels showed that several of the drawbacks associated with the pencil kernel algorithm could be significantly reduced (**Paper V**). The output factors outside the characterisation domain were found to produce less inaccurate calculations. Calculations in heterogeneous media have also been drastically improved. A remaining issue is the lack of accurate dose calculation in the build-up region. Increased dose calculation accuracy at shallow depths should offer the advantage of predicting results using *in vivo* dosimetry better.

5 Future directions

In the author's opinion, the following areas could be included in future research to further enhance dose calculation accuracy as well as facilitating TPS commissioning and verification.

5.1 Experimental methods used for verification

The methods used for experimental dose determination in this work utilized classical well-established techniques. The most common tools are small-volume detectors, e.g. ionisation chambers or silicon diodes, and extensions of these as array detectors (Leavitt and Larsson 1993). These detector types work well in beams where the fluence to each measurement point is "constant" during the beam-on time. However, as treatment delivery techniques evolve rapidly with existing equipment towards dynamic treatment, point dose detectors will have limited usefulness. They can only deliver the same amount of information as in a static beam with an extreme workload. Better dosimetry equipment, allowing simultaneous acquisition of dose data at arbitrary positions in space, must therefore be employed. While gel dosimetry has the potential to give results for large volumes (Johansson Bäck *et al.* 1998, Gustavsson *et al.* 2003), it requires the use of MR scanners for read-out. Many users have access to highly advanced dynamic delivery techniques, but do not have access to MR scanners for read-out. Although progress is being made in other read-out techniques, e.g. CT (Audet *et al.* 2002), the use of portal imaging and dose reconstruction techniques offers distinct advantages (Essers *et al.* 1996, Boellaard *et al.* 1997).

5.2 Build-up region dose calculations

Dose calculations in the build-up region have been hampered by the lack of accurate dose calculation models. This is mostly due to poor knowledge of the complex phenomena governing electron generation and transport through the treatment head to the patient. New developments that should allow for better TPS dose calculation models have, however, recently been published (Malataras *et al.* 2001, Sjögren 2001). It is important to take into account the dose due to electrons generated by the treatment head and the build-up dose at the tissue-air interface to ensure correct calculation of the dose at a point equivalent to a detector position, as is done in *in vivo* dosimetry. This will reduce the uncertainties for *in vivo* measurements and further acknowledge the

use of independent checks of the treatment administered. *In vivo* dosimetry may also be replaced by other methods as portal imaging devices are further developed. An alternative method is the use of portal imaging devices (Vallhagen Dahlgren *et al.* 2002).

5.3 Standard data sets

As many of the current TPSs still rely on measured data as input, directly or indirectly during treatment unit characterization, it would be advantageous to have a standard data set that could be used directly for dose calculations. Current linear accelerator techniques allow for matching of beam characteristics to predefined data. These data could be for a different accelerator of the same model at the same clinic or towards a standard data set as obtained from the accelerator vendor or published (Sontag and Steinberg 1999). An obvious advantage is, of course, the possibility of sharing data from investigations carried out by different user groups. Another approach to standard data is the use of Monte Carlo techniques that may simulate input data, and which can be used to create data for benchmarking the TPS, as described by Wieslander and Knöös (2000).

5.4 Monte Carlo dose calculation techniques

The model-based treatment planning system investigated here has several advantages. These include a high level of accuracy, further enhanced by the introduction of the point kernel algorithm, as well as being general enough to handle existing and future treatment techniques. As the point kernel calculation is still time-consuming even with the fast computers available today, it is not feasible to use these calculations interactively during the planning process. Although computer technology is evolving quickly, other dose calculation algorithms such as the Monte Carlo techniques, have the potential to improve treatment planning. The Monte Carlo technique could offer dose results fast with the same level of accuracy as the current state-of-the-art kernel techniques.

Acknowledgements

Most of the work for this thesis was carried out during my time at the Department of Radiation Physics (Radiofysik), Lund University Hospital, and Helax AB in Uppsala. I have met numerous people during this time and I wish to express my gratitude to everyone who has been involved in this work. If you do not find your name here, please forgive me, but space is limited.

My sincerest gratitude goes to:

Per Nilsson, for his encouragement, knowledge in radiotherapy, the time he dedicated to the current work and, last but not least, the wonderful(ly) dry martinis. Thank you.

Anders Ahnesjö, the main designer of the Helax-TMS algorithms, for his scientific skills and constant engagement.

Tommy Knöös, for his participation in this work, scientific skills and fruitful discussions.

Professor Bertil Persson, for sidetracking me into radiotherapy through all the temporary assignments at the Lund University Hospital.

My co-authors for the scientific work: Anders Ahnesjö, Tommy Knöös, Finn Laursen, Anders Murman, Per Nilsson, Mikael Saxner, Ingvar Thorslund and Erik Traneus.

The engineering team at Radiofysik for numerous repairs before, during and after my experimental sessions. Blown fuses, water in circuits where it shouldn't be, interlocks, broken X-ray tubes....

Kurt Larsson, Radiofysik, is owed considerable thanks for the excellent mechanical skills placed at my disposal over the years. Lidia Karolak, *Radiofysik*, for her professionalism and generous support in preparing the Helax-TMS clinical plans.

Everybody at Radiofysik and Helax AB (rest in peace).

John och Augusta Persson's stiftelse för vetenskaplig medicinsk forskning, Gunnar, Arvid och Elisabeth Nilsson's stiftelse för bekämpning av cancer-sjukdomar,

Lunds sjukvårdsdistrikts donationsfonder and

Svensk Förening för Radiofysik

are acknowledged for generous financial support.

Finally, on a personal level, I wish to express my gratitude to friends who have kept me away from radiation physics in numerous places such as in Nyhavn, Louisiana, Bjärred and Skrylle. Thank you Cacca and Lisa for reminding me I still had to finish this work on those occasions.

References

- Aaltonen P, Brahme A, Lax I, Levernes S, Näslund I, Reitan J B and Turesson I 1997 Specification of dose delivery in radiation therapy. Recommendation by the Nordic Association of Clinical Physics (NACP). *Acta Oncol* **36**, 1-32.
- AAPM 1983 American Association of Physicists in Medicine, A protocol for the determination of absorbed dose from high energy photon and electron beams. *Med Phys* **10**, 741-771.
- Ahnesjö A 1989 Collapsed cone convolution of radiant energy for photon dose calculation in heterogeneous media. *Med Phys* **16**, 577-592.
- Ahnesjö A 1994 Analytic modeling of photon scatter from flattening filters in photon therapy beams. *Med Phys* **21**, 1227-1235.
- Ahnesjö A 1995 Collimator scatter in photon therapy beams. *Med Phys* **22**, 267-278.
- Ahnesjö A and Andreo P 1989 Determination of effective bremsstrahlung spectra and electron contamination for photon dose calculations. *Phys Med Biol* **34**, 1451-1464.
- Ahnesjö A, Andreo P and Brahme A 1987 Calculation and application of point spread functions for treatment planning with high energy photon beams. *Acta Oncol* **26**, 49-56.
- Ahnesjö A and Aspradakis M M 1999 Dose calculations for external photon beams in radiotherapy. *Phys Med Biol* **44**, R99-155.
- Ahnesjö A, Saxner M and Trepp A 1992 A pencil beam model for photon dose calculation. *Med Phys* **19**, 263-273.

- Ahnesjö A and Trepp A 1991 Acquisition of the effective lateral energy fluence distribution for photon beam dose calculations by convolution models. *Phys Med Biol* **36**, 973-985.
- Ahnesjö A, Weber L and Nilsson P 1995 Modeling transmission and scatter for photon beam attenuators. *Med Phys* **22**, 1711-1720.
- Allen Li X, Soubra M, Szanto J and Gerig L H 1995 Lateral electron equilibrium and electron contamination in measurements of head-scatter factors using miniphantoms and brass caps. *Med Phys* **22**, 1167-1170.
- Andreo P 1990 Uncertainties in dosimetric data and beam calibration. *Int J Radiat Oncol Biol Phys* **19**, 1233-1247.
- Arnfield M R, Siantar C H, Siebers J, Garmon P, Cox L and Mohan R 2000 The impact of electron transport on the accuracy of computed dose. *Med Phys* **27**, 1266-1274.
- Audet C, Hilts M, Jirasek A and Duzenli C 2002 CT gel dosimetry technique: Comparison of a planned and measured 3D stereotactic dose volume. *J Appl Clin Med Phys* **3**, 110-118.
- Basran P S, Ansbacher W, Field G C and Murray B R 1998 Evaluation of optimized compensators on a 3D planning system. *Med Phys* **25**, 1837-1844.
- Bentzen S M 2002 "Dose-response relationships in radiotherapy". In *Basic clinical radiobiology*. Steel, G. G., Ed. (Arnold, London), pp. 94-104.
- Blomquist M, Li J, Ma C M, Zackrisson B and Karlsson M 2002 Comparison between a conventional treatment energy and 50 MV photons for the treatment of lung tumours. *Phys Med Biol* **47**, 889-897.

Boellaard B E, van Herk M and Mijnheer B J 1997 A convolution model to convert transmission dose images to exit dose distributions. *Med Phys* **24**, 189-199.

Brahme A 1984 Dosimetric precision requirements in radiation therapy. *Acta Radiol Oncol* **23**, 379-391.

Brahme A, Ed. 1988 Accuracy requirements and quality assurance of external beam therapy with photons and electrons. Stockholm, Acta Oncologica. ISBN 1100-1704.

Ceberg C P, Bjarngard B E and Zhu T C 1996 Experimental determination of the dose kernel in high-energy x-ray beams. *Med Phys* **23**, 505-511.

Chaney E L, Cullip T J and Gabriel T A 1994 A Monte Carlo study of accelerator head scatter. *Med Phys* **21**, 1383-1390.

Cunningham J R 1972 Scatter-Air Ratios. *Phys Med Biol* **17**, 42-51.

Dutreix A, Bjarngard B E, Bridier A, Mijnheer B, Shaw J E and Svensson H 1997 *Monitor Unit Calculation For High Energy Photon Beams*. (Garant Publishers, N. V., Leuven/Apeldoorn). ISBN 90-804532-2.

el-Khatib E and Battista J J 1986 Accuracy of lung dose calculations for large-field irradiation with 6-MV x rays. *Med Phys* **13**, 111-116.

Essers M, Boellaard R, van Herk M, Lanson H and Mijnheer B 1996 Transmission dosimetry with a liquid-filled electronic portal imaging device. *Int J Radiat Oncol Biol Phys* **34**, 931-941.

Essers M, Lanson J H and Mijnheer B J 1993 In vivo dosimetry during conformal therapy of prostatic cancer. *Radiother Oncol* **29**, 271-279.

Fraass B, Doppke K, Hunt M, Kutcher G, Starkschall G, Stern R and Van Dyke J 1998 American Association of Physicists in Medicine Radiation Therapy Committee Task Group 53: Quality assurance for clinical radiotherapy treatment planning. *Med Phys* **25**, 1773-1829.

Frye D M, Paliwal B R, Thomadsen B R and Jursinic P 1995 Intercomparison of normalized head-scatter factor measurement techniques. *Med Phys* **22**, 249-253.

Gustavsson H, Karlsson A, Bäck S Å J, Olsson L E, Haraldsson P, Engström P and Nyström H 2003 MAGIC-type polymer gel for three-dimensional dosimetry: Intensity-modulated radiation therapy verification. *Med. Phys.* **30**, 1264-1271.

Hurkmans C 2001 *Improvement of breast cancer irradiation techniques*. (Thesis, The Netherlands Cancer Institute, Department of Radiotherapy. Amsterdam).

Hurkmans C, Knöös T and Nilsson P 1996 Dosimetric verification of open asymmetric photon fields calculated with a treatment planning system based on dose-to-energy-fluence concepts. *Phys Med Biol* **41**, 1277-1290.

Hurkmans C, Knöös T, Nilsson P, Svahn-Tapper G and Danielsson H 1995 Limitations of a pencil beam approach to photon dose calculations in the head and neck region. *Radiother Oncol* **37**, 74-80.

IAEA 2000 Report TRS 398 *Absorbed dose determination in external beam radiotherapy. An international code of practice for dosimetry based on standards of absorbed dose to water*. (International Atomic Energy Agency. Vienna).

ICRU 1976 Report 24 *Determination of absorbed dose in a patient by beams of X or gamma rays in radiotherapy procedures*. (International Commission on Radiation Units and Measurements. Washington, DC, USA).

ICRU 1987 Report 42 *Use of computers in external beam radiotherapy procedures with high-energy photons and electrons*. (International Commission on Radiation Units and Measurements. Bethesda, MD, USA).

Jeraj R, Keall P J and Siebers J V 2002 The effect of dose calculation accuracy on inverse treatment planning. *Phys Med Biol* **47**, 391-407.

Johansson Bäck S A, Magnusson P, Fransson A, Olsson L E, Montelius A, Holmberg O, Andreo P and Mattsson S 1998 Improvements in absorbed dose measurements for external radiation therapy using ferrous dosimeter gel and MR imaging (FeMRI). *Phys Med Biol* **43**, 261-276.

Johansson K A, Karlsson R and Thilander A 1987 Report GU-RADFYS 87:13 *A small cylindric air ionization chamber with watertight protection, Type RK 83-05*. (University of Gothenburg. Gothenburg).

Johns H E and Cunningham J R 1983 *The physics of radiology*. (Charles C. Thomas, Springfield, IL). ISBN 0-398-04669-7.

Jung B, Montelius A, Dahlin H, Ekström P, Ahnesjö A, Högström B and Glimelius B 1997 The conceptual design of a radiation oncology planning system. *Comput Methods Programs Biomed* **52**, 79-92.

Kapatoes J M, Olivera G H, Reckwerdt P J, Fitchard E E, Schloesser E A and Mackie T R 1999 Delivery verification in sequential and helical tomotherapy. *Phys Med Biol* **44**, 1815-1841.

Kapatoes J M, Olivera G H, Ruchala K J and Mackie T R 2001 On the verification of the incident energy fluence in tomotherapy IMRT. *Phys Med Biol* **46**, 2953-2965.

Kase K R and Svensson G K 1986 Head scatter data for several linear accelerators (4-18 MV). *Med Phys* **13**, 530-532.

- Khan F M 1994 *The physics of radiation therapy*. (Williams and Wilkins, Baltimore, MD).
- Khan F M, Gibbons J P and Roback D M 1996 Collimator (head) scatter at extended distances in linear accelerator-generated photon beams. *Int J Radiat Oncol Biol Phys* **35**, 605-608.
- Kijewski P K, Chin L M and Bjarngard B E 1978 Wedge-shaped dose distributions by computer-controlled collimator motion. *Med Phys* **5**, 426-429.
- Knöös T, Ahnesjö A, Nilsson P and Weber L 1995 Limitations of a pencil beam approach to photon dose calculations in lung tissue. *Phys Med Biol* **40**, 1411-1420.
- Knöös T, Ceberg C, Weber L and Nilsson P 1994 The dosimetric verification of a pencil beam based treatment planning system. *Phys Med Biol* **39**, 1609-1628.
- Kutcher G J, Coia L, Gillin M, Hanson W F, Leibel S, Morton R J, Palta J R, Purdy J A, Reinstein L E, Svensson G K and et al. 1994 Comprehensive QA for radiation oncology: report of AAPM Radiation Therapy Committee Task Group 40. *Med Phys* **21**, 581-618.
- Leavitt D D and Larsson L 1993 Evaluation of a diode detector array for measurement of dynamic wedge dose distributions. *Med Phys* **20**, 381-382.
- Levene M B, Kijewski P K, Chin L M, Bjarngard B E and Hellman S 1978 Computer-controlled radiation therapy. *Radiology* **129**, 769-775.
- Lewis R D, Ryde S J, Seaby A W, Hancock D A and Evans C J 2000 Use of Monte Carlo computation in benchmarking radiotherapy treatment planning system algorithms. *Phys Med Biol* **45**, 1755-1764.

Mackie T R, Reckwerdt P, McNutt T, Gehring M and Sanders C 1996 "Photon beam dose computations". In *Teletherapy: Present and future*. Mackie, T. R. and Palta, J. R., Eds. (Advanced Medical Publishing, Madison, WI, USA), pp. 103-135.

Mackie T R, Scrimger J W and Battista J J 1985 A convolution method of calculating dose for 15 MV x-rays. *Med Phys* **12**, 327-332.

Malataras G, Kappas C and Lovelock D M 2001 A monte carlo approach to electron contamination sources in the Saturne-25 and -41. *Phys Med Biol* **46**, 2435-2446.

Mijnheer B J, Battermann J J and Wambersie A 1987 What degree of accuracy is required and can be achieved in photon and neutron therapy? *Radiother Oncol* **8**, 237-252.

Mohan R, Chui C and Lidofsky L 1986 Differential pencil beam dose computation model for photons. *Med Phys* **13**, 64-73.

O'Connor J E and Malone D E 1989 A cobalt-60 primary dose spread array derived from measurements. *Phys Med Biol* **34**, 1029-1042.

Saxner M and Ahnesjö A 1998 Implementation of the collapsed cone method for clinical beam qualities. *Med Phys* **25**, A185.

SGSMP 1997 Report SGSMP Report 7 *Quality control of treatment planning systems for teletherapy*. (Swiss Society for Radiobiology and Medical Physics (SGSMP/SSRPM/SSRFM)).

Shih R, Lj X A and Hsu W L 2001 Dosimetric characteristics of dynamic wedged fields: a Monte Carlo study. *Phys Med Biol* **46**, N281-292.

Sjögren R 2001 *Electron contamination of photon beams*. (Thesis, Umeå University, Department of Radiation Sciences. Umeå).

- Sontag M R and Steinberg T H 1999 Performance and beam characteristics of the Siemens Primus linear accelerator. *Med Phys* **26**, 734-736.
- Spezi E, Lewis D G and Smith C W 2001 Monte Carlo simulation and dosimetric verification of radiotherapy beam modifiers. *Phys Med Biol* **46**, 3007-3029.
- Spicka J, Herron D and Orton C 1988 Separating output factor into collimator factor and phantom scatter factor for megavoltage photon calculations. *Med Dosim* **13**, 23-24.
- Steel G G, Ed. 2002 Basic clinical radiobiology. London, Arnold. ISBN 0 340 80783 0.
- Stewart B W and Kleihues P, Eds. 2003 World cancer report. Lyon, IARC Press. ISBN 92 832 0411 5.
- Storchi P R, van Battum L J and Woudstra E 1999 Calculation of a pencil beam kernel from measured photon beam data. *Phys Med Biol* **44**, 2917-2928.
- Tatcher M and Bjarngard B E 1993 Head-scatter factors in rectangular photon fields. *Med Phys* **20**, 205-206.
- Vallhagen Dahlgren C, Ahnesjö A, Montelius A and Rikner G 2002 Portal dose image verification: formalism and application of the collapsed cone superposition method. *Phys Med Biol* **47**, 4371-4387.
- van Bree N A, van Battum L J, Huizenga H and Mijnheer B J 1991 Three-dimensional dose distribution of tangential breast treatment: a national dosimetry intercomparison. *Radiother Oncol* **22**, 252-260.
- Van Dyk J, Barnett R B, Cygler J E and Shragge P C 1993 Commissioning and quality assurance of treatment planning computers. *Int J Radiat Oncol Biol Phys* **26**, 261-273.

van Gasteren J J, Heukelom S, van Kleffens H J, van der Laarse R, Venselaar J L and Westermann C F 1991 The determination of phantom and collimator scatter components of the output of megavoltage photon beams: measurement of the collimator scatter part with a beam-coaxial narrow cylindrical phantom. *Radiother Oncol* **20**, 250-257.

Weber L, Murman A and Ahnesjö A 2001 Variability of clinical beam data for commissioning of treatment planning systems. *Radiother Oncol* **61**, S88.

Venselaar J, Welleweerd H and Mijnheer B 2001 Tolerances for the accuracy of photon beam dose calculations of treatment planning systems. *Radiother Oncol* **60**, 191-201.

Wieslander E and Knöös T 2000 A virtual linear accelerator for verification of treatment planning systems. *Phys Med Biol* **45**, 2887-2896.

Populärvetenskaplig sammanfattning

Framgångsrik strålbehandling av cancerpatienter kräver att man kan bestämma den absorberade dosen i patienten med stor noggrannhet. Bara några enstaka procents avvikelser i absorberad dos kan ha betydelse för det kliniska resultatet avseende både tumörtläkning och normalvävnadsreaktioner.

För att beräkna den absorberade dosen i patienten används sofistikerade datorprogram, som tillsammans med hårdvaran i dagligt tal kallas ”dosplaneringssystem”. Moderna beräkningsmetoder är baserade på s.k. energideponeringskärnor som beskriver den absorberade dosen i vatten kring antingen en enda växelverkanpunkt (punktspridningsfunktion) eller alternativt längs en smal stråle. Med hjälp av dessa kärnor kan sedan den absorberade dosfördelningen i patienten beräknas.

I detta arbete har ett dosplaneringssystem, Helax-TMS, baserat på energideponeringskärnor, studerats. Systemet är det vanligast förekommande på svenska strålbehandlingsavdelningar. Inom ramen för arbetet har vi studerat den noggrannhet med vilken den absorberade dosfördelningen kan beräknas i olika situationer. Metoden som använts har varit att jämföra beräkningar i dosplaneringssystemet mot experimentella mätningar i vatten i identiska geometrier. Detta har fördelen att det är lätt att jämföra med dosplaneringsberäkningar samt med resultat från andra undersökningar eftersom detta är den gängse teknik som använts tidigare. Undantaget har varit fall där det är förknippat med experimentella svårigheter att mäta absorberad dos, exempelvis i områden motsvarande vävnader med täthet skild från mjukvävnad. I dessa fall har simuleringar med s.k. Monte Carlo teknik använts.

De områden som fokuserats på i denna studie har varit vanligt förekommande tekniker i samband med strålbehandling; öppna och kilade fält samt i samband med dessa; asymmetriska fält och geometrier med varierande vävnadstäthet. Olika behandlingstekniker som kompensationsfilter och kilfält genererade av kollimatorer i rörelse, s.k. dynamiska kilar, har också undersökts.

Resultaten visar att beräkningsmodellerna i Helax-TMS uppfyller allmänt accepterade krav i de flesta situationerna. För de flesta undersökta fallen har avvikelserna i absorberad dos varit inom intervallet $\pm 3\%$.

